Numerical Modelling of Solar Heat Storage Using Large Arrays of Borehole Heat Exchangers

H.-J.G. Diersch [1], W. Rühaak [1], P. Schätzl [1], D. Bauer [2] , W. Heidemann [2]

[1] DHI-WASY GmbH, Waltersdorfer Straße 105, 12526 Berlin Germany

[2]Institute of Thermodynamics and Thermal Engineering, University of Stuttgart

w.ruehaak@dhi-wasy.de

Keywords: Numerical modeling, heat transport, borehole heat exchangers, solar heat storage

ABSTRACT

The storage of surplus heat in the underground and retrieval when required is a promising method for optimizing the energy efficiency of new housing estates. A new approach for the coupled numerical modelling of such problems will be presented. Here, the energy simulation software TRNSYS is directly coupled with the finite element subsurface flow and transport simulation software FEFLOW. This way it is possible to simulate the energy transfer between solar panels, building installations and thermal storage in the subsurface in an efficient and accurate manner. At the presented pilot installation the heat is transferred to the ground by using large arrays of borehole heat exchangers. For the simulation the borehole heat exchanger systems are modeled by a set of one-dimensional representations, either using a finite-element or an analytical approach. This way the calculation time is significantly reduced compared to fully discretized calculations while still achieving precise results.

1. INTRODUCTION

Shallow geothermics has an increasing importance worldwide. Expertise on environmental matters requires estimating the potential impact of Borehole Heat Exchanger (BHE) systems on the subsurface temperature. Various techniques are available to analyze the flow and heat transport processes for BHE and the surrounding soil layers. Currently, two major approaches are preferred. First, BHE is modelled in a fully discretized manner via numerical schemes in three dimensions. However, due to the extreme disproportional geometries and high parametric contrasts typical for BHE the computation becomes a difficult and expensive numerical task. Second, analytical or semi-analytical techniques have shown attractive in engineering practice. However, their results are restricted due to inherent simplified assumptions (e.g., averaged quantities, neglecting groundwater interaction, linearization of underlying physics). As a result, more efficient and powerful methods are required providing the full coupling between BHE and the subsurface without the need to resolve BHE in geometric detail. This becomes especially important in the case of large BHE arrays.

BHE systems can be constructed in different ways. The most common in practice are single U-shape pipe (consisting of an inlet pipe, an outlet pipe and grout), double U-shape pipe (consisting of two inlet pipes, two outlet pipes and grout) and coaxial pipe (consisting of an inlet pipe included with an outlet pipe and grout) installations. Such heat exchangers form a vertical borehole system, where a refrigerant circulates in closed pipes exchanging heat with the surrounding aquifer driven alone by thermal conductivity (closed loop system). However, the extreme slenderness, typically involved in those boreholes, requires an advanced numerical strategy, where the BHE systems are modelled by 1D finite-element representations. We mainly follow the ideas proposed by Al-Khoury et al. (2005) and Al-Khoury and Bonnier (2006), who firstly used 1D single and double U-pipe elements in the context of geothermal heating systems. Al-Khoury et al.'s numerical strategy is further modified and adapted to FEFLOW (Diersch and Kolditz, 2002, Zheng, 2007) with respect to the following:

- Integrating the 1D BHE pipe elements into FEFLOW's finite-element matrix system similar to fracture elements.

- Generalization of the formulations for single and double U-shape as well as coaxial pipe configurations.

- Direct and non-sequential (essentially non-iterative) coupling of the 1D pipe elements to the porous medium discretization.

- Extending FEFLOW's boundary conditions for BHE pipes similar to multi-well borehole conditions.

2. BOREHOLE HEAT EXCHANGER

The following numerical procedures are given for the double U-shape pipe (2U) exchanger, but can be easily translated to other BHE types. The 2U is a cylindrical borehole consisting of two inner pipes forming a U-shape and filled with a grout material as shown in Figure 2.

There are eight components of a 2U exchanger:

- two pipes-in (denoted as *i1* and *i2*)

- two pipes-out (denoted as *o1* and *o2*)

- grout material which is subdivided into 4 zones (denoted as g1, g2, g3, g4)

The four pipe components *i1, i2, o1,* and *o2* transfer heat across their cross-sectional areas and exchange fluxes across their surface areas. The radial heat transfer from the pipes is directed to the grout zones g_i (i=1,...,4). The grout zones g_i exchange heat directly to the surrounding soil (the porous matrix with the filled fluid in the void space) denoted as *s* and to other contacted grout zones, too. The heat coupling only occurs via the grout zones, which work as intermediate media that transfer heat from one pipe to another and vice versa. Only the grout zones exchange heat with the surrounding soil *s*. The 2U system involves several material and geometrical parameters, which are either given by the manufacturer of the heating systems or determined experimentally. These relations are used to express the overall thermal resistance between the 2U borehole and the soil. The usual practice is to lump the effects of the 2U components into effective heat transfer coefficients

representing the reciprocal of the sum of the thermal resistances between the different components. The inner pipe-grout heat flux resistance relationships are shown in Figure 2. Their analytical descriptions will be given below.

2.1 Formulation of the Soil Equations

2.1.1 Basic Equations

The conservation equation of fluid mass is given by

$$S_0 \frac{\partial h}{\partial t} + \nabla \cdot \mathbf{q} = Q + Q_{EOB} \tag{1}$$

where S_0 is specific storage coefficient (m^{-1}), h is hydraulic head (m), t is time (s), Q is flow supply (s^{-1}). The flux $\mathbf{q}$ (m s^{-1}) in the porous medium is expressed by the Darcy law as

$$\mathbf{q} = -\mathbf{K}(\nabla h + \psi) \tag{2}$$

$\mathbf{K}$ (m s^{-1}) represents the hydraulic conductivity tensor given by

$$\mathbf{K} = \frac{\mathbf{k}\rho_0^f |\mathbf{g}|}{\mu_0^f} \tag{3}$$

where $\mathbf{k}$ is permeability tensor (m^2), ρ^f is fluid density (kg m^{-3}) and $\mathbf{g}$ is the gravity vector (m s^{-2}). The temperature dependence of the dynamic viscosity μ^f (kg m^{-1} s^{-1}) can also be taken into account. Superscript f stands for fluid. ψ is the buoyancy term calculated as

$$\psi = \frac{\rho^f - \rho_0^f}{\rho_0^f} \cdot \frac{-\mathbf{g}}{|\mathbf{g}|}, \text{ and}$$
$$\rho^f = \rho_0^f [1 - \beta(T_s - T_{s0})] \tag{4}$$

where β is the thermal expansion coefficient (°C^{-1}) and T is temperature (°C). Subscript s stands for soil and 0 for a reference value.

The extended Oberbeck-Boussinesq approximation is calculated as

$$Q_{EOB} = \beta \left(q \cdot \nabla T_s + \varepsilon \frac{\partial T_s}{\partial t} \right) \tag{5}$$

where ε is porosity (-).

The conservation equation of thermal energy in the soil s can be expressed as

$$\frac{\partial (\rho c)^b T_s}{\partial t} + \nabla \cdot \left((\rho c)^f \mathbf{q} T_s \right) - \nabla \cdot (\mathbf{\Lambda} \cdot \nabla T_s) = H_s \tag{6}$$

with the tensor of thermal hydrodynamic dispersion

$$\mathbf{\Lambda} = \lambda^b \mathbf{I} + (\rho c)^f \left[\alpha_T \|\mathbf{q}\| \mathbf{I} + (\alpha_L - \alpha_T) \frac{\mathbf{q} \otimes \mathbf{q}}{\|\mathbf{q}\|} \right] \tag{7}$$

Here α_L and α_T (m) are longitudinal and transverse thermo-dispersivity, respectively, $\mathbf{I}$ is unit vector (-), c is specific heat capacity (J kg^{-1} K^{-1}), λ is thermal conductivity (W K^{-1} m^{-1}) and H (W m^{-3}) is thermal sink/source term. Superscript b denotes bulk values. Thermal boundary conditions of Dirichlet-, Neumann- and Cauchy-type can be applied as usual.
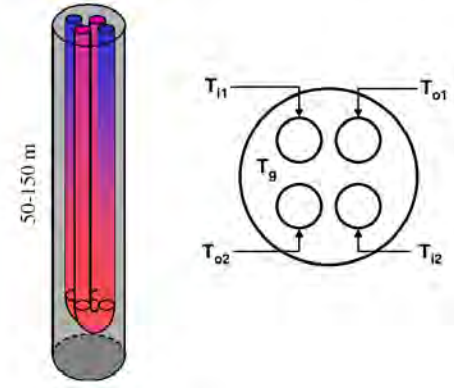

Figure 1: Schematization of a 2U-type BHE (from Al-Khoury and Bonnier, 2006)
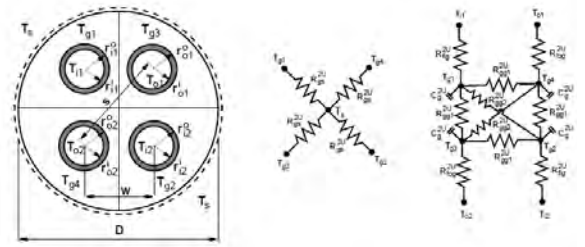

Figure 2: Inner pipe-grout heat flux resistance relationships of a 2U borehole

2.22.2 Pipe equations

2.2.1 Basic equations

The BHE represents a closed pipe system, where a refrigerant fluid is circulating with a given velocity $\mathbf{u}$. The heat transport equations of a 2U configuration can be written for the inflow pipe $i1$ as follows

$$\frac{\partial}{\partial t}(\rho^r c^r T_{i1}) + \nabla \cdot (\rho^r c^r \mathbf{u} T_{i1}) - \nabla \cdot (\mathbf{\Lambda}^r \cdot \nabla T_{i1}) = H_{i1} \quad \text{in} \quad \Omega_{i1} \tag{8}$$
$$\text{with} \quad \mathbf{q}_{nT_{i1}} = -\Phi_{fig}(T_{g1} - T_{i1}) \quad \text{on} \quad \Gamma_{i1}$$

and similarly for $i2$, $o1$ and $o2$. The grout equation for g1 reads

$$\frac{\partial}{\partial t}(\varepsilon_g \rho^g c^g T_{g1}) - \nabla \cdot (\varepsilon_g \lambda^g \nabla T_{g1}) = H_{g1} \quad \text{in} \quad \Omega_{g1}$$
$$\text{with} \tag{9}$$
$$\mathbf{q}_{nT_{g1}} = -\Phi_{gs}(T_s - T_{g1}) - \Phi_{fig}(T_{i1} - T_{g1}) -$$
$$\Phi_{gg2}(T_{g2} - T_{g1}) - \Phi_{gg1}(T_{g3} - T_{g1})$$
$$- \Phi_{gg1}(T_{g4} - T_{g1}) \quad \text{on} \quad \Gamma_{g1}$$

Similarly for g2, g3 and g4, where

$$\mathbf{\Lambda}^r = (\lambda^r + \rho^r c^r \alpha_L \|\mathbf{u}\|) \mathbf{I} \tag{10}$$

For single U-shape pipe and coaxial pipe exchangers only four respectively three borehole components exist consisting of one pipe-in, one pipe-out and two respectively one grout zone(s). In these cases the equations for the second in-/outflow are irrelevant and the transfer coefficients for the second pipe vanish.

2.2.2 Heat transfer coefficients

Thermal resistances are determined from the physical, material and geometric engineering parameters of the different BHE configurations as shown in Fig. 2 for the 2U exchanger. As indicated there the interaction between the

different components of the pipe exists between the pipe-in and grout zones, the pipe-out and grout zones as well as the pipe-in and pipe-out. The following thermal resistances can be derived.

The thermal resistance between the pipes and grout zones is caused by the advection of the pipe flow and thermal conductivity of the pipe wall material specified separately for pipe-in and pipe-out

$$R_{\bar{f}ig} = R_{adv_k} + R_{con_k^a} + R_{con^b} \quad (k = i1 \cap i2), \tag{11}$$

And similarly for R_{fog}.

Thermal resistance due to the advective flow of refrigerant in the pipes

$$R_{adv_k} = \frac{1}{Nu_k \lambda^r \pi} \quad (k = i1, o1, i2, o2) \tag{12}$$

In (12) the Nusselt numbers, Nu_k, differ between laminar and turbulent flow (VDI, 2006), $viz.$,

for laminar flow if $Re_k < 2300$
$$Nu_k = 4.364$$
for turbulent flow if $Re_k \geq 10^4$

$$Nu_k = \frac{(\xi_k/8) Re_k \, Pr}{1 + 12.7\sqrt{\xi_k/8}\left(Pr^{2/3} - 1\right)}\left[1 + \left(\frac{D_k^i}{\bar{L}}\right)^{2/3}\right] \tag{13}$$

for flow in transition range if $2300 \leq Re_k < 10^4$
$$Nu_k = (1 - \gamma_k)4.364 +$$
$$\gamma_k \left\{ \frac{(0.0308/8)10^4 \, Pr}{1 + 12.7\sqrt{0.0308/8}\left(Pr^{2/3} - 1\right)}\left[1 + \left(\frac{d_k^i}{L}\right)^{2/3}\right] \right\}$$

in which Pr represents the Prandtl number and Re_k are the Reynolds number defined as

$$Pr = \frac{\mu^r c^r}{\lambda^r} \qquad Re_k = \frac{|\mathbf{u}| d_k^i}{\mu^r / \rho^r} \qquad (k = i1, o1, i2, o2) \tag{14}$$

Where d_k^i are the diameters of the pipes $d_k^i = 2r_k^i \ (k = i1, o1, i2, o2)$. Furthermore, $\bar{L}$ corresponds to the length of the pipe and

$$\xi_k = (1.8 \log_{10} Re_k - 1.5)^{-2} \tag{15}$$
$$\gamma_k = \frac{Re_k - 2300}{10^4 - 2300} \qquad (0 \leq \gamma_k \leq 1)$$

It is

$$|\mathbf{u}_k| = \begin{cases} \dfrac{Q_r}{2\pi(r_k^i)^2} & \text{for parallel discharge} \\ \dfrac{Q_r}{\pi(r_k^i)^2} & \text{for serial discharge} \end{cases}, (k = i1, o1, i2, o2) \tag{16}$$

Thermal resistances due to the pipes wall material and grout transition

$$R_{con_k^a} = \frac{\ln(r_k^a / r_k^i)}{2\pi\lambda_k^p} \qquad (k = i1, o1, i2, o2) \tag{17}$$

Where λ_k^p corresponds to the thermal conductivities of the pipe wall material.

$$R_{con^b} = xR_g \tag{18}$$

with

$$x = \frac{\ln\left(\frac{\sqrt{D^2 + 4d_o^2}}{2\sqrt{2}d_o}\right)}{\ln\left(\frac{D}{2d_o}\right)} \tag{19}$$

and

$$R_g = \frac{\operatorname{arcosh}\left(\frac{D^2 + d_o^2 - s^2}{2Dd_o}\right)}{2\pi\lambda^g}\left(3.098 - 4.432\frac{s}{D} + 2.364\frac{s^2}{D^2}\right) \tag{20}$$

Where D denotes the borehole diameter, $d_o = \frac{1}{4}\sum_k d_k^o$ is the averaged outer diameter of the pipes $d_k^o = 2r_k^o \ (k = i1, o1, i2, o2)$ and $s = w\sqrt{2}$ corresponds to the diagonal distance of the pipes (see Fig. 2)

Thermal resistance due to inter-grout exchange:

$$R_{gg1} = \frac{2R_{gs}(R_{ar1} - 2xR_g)}{2R_{gs} - R_{ar1} + 2xR_g}; R_{gg2} = \frac{2R_{gs}(R_{ar2} - 2xR_g)}{2R_{gs} - R_{ar2} + 2xR_g} \tag{21}$$

with

$$R_{ar1} = \frac{\operatorname{arcosh}\left(\frac{s^2 - d_o^2}{d_o^2}\right)}{2\pi\lambda^g}; R_{ar2} = \frac{\operatorname{arcosh}\left(\frac{2s^2 - d_o^2}{d_o^2}\right)}{2\pi\lambda^g}. \tag{22}$$

Thermal resistance due to the grout material is:

$$R_{gs} = (1 - x)R_g \tag{23}$$

The heat transfer coefficients specified for the 2U configuration are related to thermal resistance relationships. Due to the analogy of Fourier's law for heat flow and Ohm's law for electric current flow simple formulations can be derived to lump the effects of the BHE constituents into an effective coefficient representing the reciprocal of the sum of the thermal resistances acting on their specific exchange surfaces S between the different components.

$$\Phi_{fig} = \frac{1}{R_{fig}}\frac{1}{S_i}; \Phi_{fog} = \frac{1}{R_{fog}}\frac{1}{S_o};$$
$$\Phi_{gg1} = \frac{1}{R_{gg1}}\frac{1}{S_{g1}}; \Phi_{gg2} = \frac{1}{R_{gg2}}\frac{1}{S_{g2}}; \tag{24}$$
$$\Phi_{gs} = \frac{1}{R_{gs}}\frac{1}{S_{gs}}$$

2.3 Analytical BHE Solution

2.3.1 Local Steady-State Condition with Given Temperature at Borehole Wall

The present analytical solution is only valid for local steady-state heat transport and a given temperature Ts at borehole wall. It was first derived by Eskilson and Claesson (1988) for heat transfer between two pipes and the borehole wall. We extend the analytical method to coaxial pipe with annular (CXA) and centred (CXC) inlet, 1U and 2U configurations of BHE. The local steady-state heat balance equations for fluid in pipe-in and pipe-out reads

Diersch et al.

$$-A^i \rho^r c^r u\left(\nabla_z T_{i1}\right) = \frac{T_{i1}-T_s}{R_1^\Delta} + \frac{T_{i1}-T_{o1}}{R_{12}^\Delta} \quad (25)$$

$$A^i \rho^r c^r u\left(\nabla_z T_{o1}\right) = \frac{T_{o1}-T_s}{R_2^\Delta} + \frac{T_{o1}-T_{i1}}{R_{12}^\Delta}$$

which have to be solved for the pipe(s)-in temperature $T_{i1}(z)$ and pipe(s)-out temperature $T_{o1}(z)$. The vertical heat conductivity in the pipes is neglected. It is further assumed that the inner cross-sectional area of pipe-in and pipe-out is equal $A^i = A_i^i = A_o^i$. The local steady-state condition limits the application of (20) to a time scale larger than

$$t > t_{\lim it}^{steady} = \frac{5}{4}D^2\left(\frac{\varepsilon \rho^f c^f + (1-\varepsilon)\rho^s c^s}{\varepsilon \lambda^f + (1-\varepsilon)\lambda^s}\right) \quad (26)$$

The time for the refrigerant to circulate through the borehole is $2A^i \overline{L}/Q_r$. Accordingly, equations (20) can only describe transient input variations of inlet temperature and pumping rate on a time scale larger than

$$t > t_{\lim it}^{steady} + A^i \frac{2\overline{L}}{Q_r} \quad (27)$$

The specific thermal flux $\varphi(z,t)$ exchanging heat of the borehole with the adjacent soil s is given from (20) according to

$$\varphi(z,t) = \frac{T_s - T_{i1}}{R_1^\Delta} + \frac{T_s - T_{o1}}{R_2^\Delta} \quad (28)$$

2.3.2 Eskilson and Claesson's Analytical BHE Solution

The coupled equations (76) can be solved by using Laplace transforms (Eskilson and Claesson, 1988). It yields

$$T_{i1}(z) = T_{i1}(0)f_1(z) + T_{o1}(0)f_2(z) + T_s\int_0^z f_4(z-\xi)d\xi$$
$$(0 \leq z \leq \overline{L}) \quad (29)$$
$$T_{o1}(z) = T_{i1}(0)f_2(z) + T_{o1}(0)f_3(z) + T_s\int_0^z f_5(z-\xi)d\xi$$

The functions $f_1, f_2, \ldots, f_5$ are given by the expressions

$$f_1(z) = e^{\beta z}\left[\cosh(\gamma z) - \delta\sinh(\gamma z)\right]$$
$$f_2(z) = e^{\beta z}\frac{\beta_{12}}{\gamma}\sinh(\gamma z) \quad (30)$$
$$f_3(z) = f_1(z)$$
$$f_4(z) = e^{\beta z}\left[\beta_1\cosh(\gamma z) - \left(\delta\beta_1 + \frac{\beta_2\beta_{12}}{\gamma}\right)\sinh(\gamma z)\right]$$
$$f_5(z) = e^{\beta z}\left[\beta_2\cosh(\gamma z) + \left(\delta\beta_2 + \frac{\beta_1\beta_{12}}{\gamma}\right)\sinh(\gamma z)\right]$$

where

$$\beta_1 = \frac{1}{R_1^\Delta A^i \rho^r c^r u} \quad \beta_2 = \frac{1}{R_2^\Delta A^i \rho^r c^r u}$$
$$\beta_{12} = \frac{1}{R_{12}^\Delta A^i \rho^r c^r u} \quad \beta = \frac{\beta_2 - \beta_1}{2} \quad (31)$$
$$\gamma = \sqrt{\frac{(\beta_1-\beta_2)^2}{4} + \beta_{12}(\beta_1-\beta_2)}$$
$$\delta = \frac{1}{\gamma}\left(\beta_{12} + \frac{\beta_1-\beta_2}{2}\right)$$

The following boundary conditions are applied

$$T_{i1}(0) = T$$
$$T_{i1}(\overline{L}) = T_{o1}(\overline{L}) \quad (32)$$

where T_i represents the inlet temperature. Using (32) in (30) and (31) the outlet temperature T_o is given as

$$T_o = T_{o1}(0) \quad (33)$$

2.3.3 Solution for a 2U Configuration

It is assumed that the pipes are arranged symmetrically within the borehole. Accordingly, there is

$$R_2^\Delta = R_1^\Delta \quad (34)$$

so that

$$\beta_2 = \beta_1 = \frac{1}{R_1^\Delta A^i \rho^r c^r u}$$
$$\beta_{12} = \frac{1}{R_{12}^\Delta A^i \rho^r c^r u}$$
$$\beta = 0 \quad (35)$$
$$\gamma = \sqrt{\beta_1^2 + 2\beta_{12}\beta_1}$$
$$\delta = \frac{1}{\gamma}(\beta_{12} + \beta_1)$$

Hence, (30) simplifies

$$f_1(z) = \cosh(\gamma z) - \delta\sinh(\gamma z)$$
$$f_2(z) = \frac{\beta_{12}}{\gamma}\sinh(\gamma z) \quad (36)$$
$$f_3(z) = f_1(z)$$
$$f_4(z) = \beta_1\cosh(\gamma z) - \left(\delta\beta_1 + \frac{\beta_2\beta_{12}}{\gamma}\right)\sinh(\gamma z)$$
$$f_5(z) = \beta_2\cosh(\gamma z) + \left(\delta\beta_2 + \frac{\beta_1\beta_{12}}{\gamma}\right)\sinh(\gamma z)$$

In using (32) the equations (29) can be equalized at $z = \overline{L}$ and solved for the outlet temperature T_o, viz.,

$$T_0 = T_i\frac{f_1(z)+f_2(z)}{f_3(z)-f_2(z)} +$$
$$\frac{T_s}{f_3(z)-f_2(z)}\int_0^{\overline{L}}[f_1(z-\xi)+f_5(z-\xi)]d\xi \quad (37)$$
$$= T_i\frac{f_1(z)+f_2(z)}{f_3(z)-f_2(z)} + \frac{T_s}{f_3(z)-f_2(z)}\frac{2\beta}{\gamma}\sinh(\gamma z)$$
applied to $z = \overline{L}$

With known inlet temperature T_i from the boundary condition (32) and outlet temperature T_o from (37) the temperature distributions T_{i1} and T_{o1} as a function of z are obtained after evaluating the integrals in (29). It yields

$$T_{i1}(z) = T_i f_1(z) + T_o f_2(z) +$$
$$T_s\frac{\beta_1}{\gamma}\left[\left(\delta + \frac{\beta_{12}}{\gamma}\right)(1-\cosh(\gamma z) + \sinh(\gamma z))\right] \quad (38)$$
$$T_{o1}(z) = -T_i f_2(z) + T_o f_3(z) +$$
$$T_s\frac{\beta_1}{\gamma}\left[\left(\delta + \frac{\beta_{12}}{\gamma}\right)(1-\cosh(\gamma z) + \sinh(\gamma z))\right]$$

The temperature distribution for the grout zones $T_{g1}(z)$ and $T_{g2}(z)$ can be derived for the 2U configuration as

$$T_{g1}(z) = T_{g2}(z) = \frac{\left[\dfrac{2T_s}{R_{gs}^{2U}} + \dfrac{2T_{o1}(z)}{R_{fig}^{2U}} + \left(\dfrac{2T_s}{R_{gs}^{2U}} + \dfrac{2T_{i1}(z)}{R_{fig}^{2U}}\right)u_2 v\right]v}{v^2 u_2^2 - 1} \quad (39)$$

$$T_{g3}(z) = T_{g4}(z) = \left(\frac{T_{g1}(z)}{v} + \frac{2T_{o1}(z)}{R_{fig}^{2U}} + \frac{2T_s}{R_{gs}^{2U}}\right)\frac{1}{u_2}$$

with

$$u_2 = \frac{2}{R_{fig}^{2U}} + \frac{2}{R_{gs}^{2U}} + \frac{1}{v} \quad (40)$$

$$v = \frac{R_{gg1}^{2U} R_{gg2}^{2U}}{2\left(R_{gg1}^{2U} + R_{gg2}^{2U}\right)}$$

The thermal resistances R_1^Δ and R_{12}^Δ are given by

$$R_1^\Delta = \frac{R_{fig}^{2U} + R_{gs}^{2U}}{2} \quad (41)$$

$$R_{12}^\Delta = \frac{\left(R_{fig}^{2U}\right)^2}{4}\left(u_2^2 v - \frac{1}{v}\right)$$

for 2U pipes.

2.4 Implementation

The finite element discretization yields a matrix system, which can be written in compact form as

$$\begin{bmatrix} \mathbf{A}_{pipe} & \mathbf{R}_{ps} \\ \mathbf{R}_{ps}^T & \mathbf{A}_s \end{bmatrix} \cdot \begin{Bmatrix} \mathbf{T}_{pipe} \\ \mathbf{T}_s \end{Bmatrix} = \begin{Bmatrix} \mathbf{B}_{pipe} \\ \mathbf{B}_s \end{Bmatrix} \quad (42)$$

where subscripts *pipe* and *s* denote entities for the inner pipe problem and the outer soil problem, respectively, while subscript *ps* identifies pipe-soil transfer entities. To solve the matrix system (42) a static condensation strategy (Zienkiewicz and Taylor, 2000) is applied. In doing this, a reduced equation system results

$$\begin{aligned} \left(\mathbf{A}_s - \mathbf{A}_{ps}\right)\cdot\mathbf{T}_s &= \mathbf{B}_s - \mathbf{B}_{ps} \\ \mathbf{A}_{ps} &= \mathbf{R}_{ps}^T\cdot\left(\mathbf{A}_{pipe}^{-1}\cdot\mathbf{R}_{ps}\right) \\ \mathbf{B}_{ps} &= \mathbf{R}_{ps}^T\cdot\left(\mathbf{A}_{pipe}^{-1}\cdot\mathbf{R}_{pipe}\right) \end{aligned} \right\} \quad (43)$$

for solving only the soil temperature $\mathbf{T}_s$. Using Eq. (42) a direct and non-sequential solution of the complete temperature field for the soil and the pipe is possible.

2.5 Implementation Analytical BHE Solution

For the soil temperatures $T_s^{n+1} = T_s\left(t^{n+1}\right)$ the spatio-temporal finite element discretization is taken in the following form:

$$\left([\mathbf{A}_s *] + [\mathbf{R}_{BHE}]\right)\cdot\{\mathbf{T}_s\}^{n+1} = \{\mathbf{B}_s\}^{n+1} + \left\{\mathbf{B}_{BHE}\left(\mathbf{T}_s^{n+1}\right)\right\} \quad (44)$$

where with (28) a BHE-related diagonal resistance matrix

$$\mathbf{R}_{BHE} = \int_z \left(\frac{1}{R_1^\Delta} + \frac{1}{R_2^\Delta}\right)dz\mathbf{I} \quad (45)$$

and a source/sink term on the RHS

$$\mathbf{B}_{BHE}\left(\mathbf{T}_s^{n+1}\right) = \int_z \left(\frac{\mathbf{T}_{i1}^{n+1}}{R_1^\Delta} + \frac{\mathbf{T}_{o1}^{n+1}}{R_2^\Delta}\right)dz\mathbf{I} \quad (46)$$

appear. The temperature distributions for pipe(s)-in $\mathbf{T}_{i1}^{n+1}$ and pipe(s)-out $\mathbf{T}_{o1}^{n+1}$ represent complex analytical

expressions as given in the previous text (see equation 38). Since they are again dependent on the soil temperature

$$\begin{aligned} \mathbf{T}_{i1}^{n+1} &= \mathbf{T}_{i1}^{n+1}\left(\mathbf{T}_s^{n+1}\right) \\ \mathbf{T}_{o1}^{n+1} &= \mathbf{T}_{o1}^{n+1}\left(\mathbf{T}_s^{n+1}\right) \end{aligned} \quad (47)$$

the matrix system (44) is solved via an iterative procedure according to

starting solution $\tau = 0$
$$\left([\mathbf{A}_s *] + \mathbf{R}_{BHE}\right)\cdot\{\mathbf{T}_s\}^{(n+1),\tau} = \{\mathbf{B}_s\}^{n+1} + \left\{\mathbf{B}_{BHE}\left(\mathbf{T}_s^n\right)\right\}$$
iteration $\tau + 1$
$$\left([\mathbf{A}_s *] + \mathbf{R}_{BHE}\right)\cdot\{\mathbf{T}_s\}^{(n+1),(\tau+1)} = \{\mathbf{B}_s\}^{n+1} + \left\{\mathbf{B}_{BHE}\left(\mathbf{T}_s^{(n+1),\tau}\right)\right\}$$
$$(48)$$

The iterations with the current time level (n +1) are stopped if

$$\left\|T_s^{(n+1),(\tau+1)} - T_s^{(n+1),\tau}\right\|_{L_p} < \delta \quad (49)$$

2.6 Model Validation

2.6.1 Analytical Solution of Heat Transport in a Single Pipe with Soil Interaction

Exact solutions for heat flow in BHE configurations imbedded in a 3D layered soil system do not exist. However, there are analytical solutions suited for the partial problem of the 1D heat transport in a single pipe with a lateral heat exchange to the surrounding grout or soil. It can be used to compare the numerical results for a BHE solution at a starting period when the heat flow develops in the 1D pipe-in of a heat exchanger interacting with soil. It is assumed that the heat transfers to the grout and to the soil are equal. In such a case the governing heat transport equation reads

$$\frac{\partial T}{\partial t} + u\frac{\partial T}{\partial z} - D\frac{\partial^2 T}{\partial z^2} + \phi(T - T_s) = 0 \quad (50)$$

where T ($=T_{i1}$) is the fluid temperature in the pipe-in, u is the refrigerant fluid velocity, D is the thermal diffusivity, ϕ is a specific heat transfer coefficient, T_s is the surrounding soil temperature taken as a reference temperature and z is the vertical coordinate. Thermo-dispersivity, refrigerant fluid velocity and specific heat transfer coefficient are related to the parameters used in the numerical modelling as follows:

$$D = \frac{|\Lambda^r|}{\rho^r c^r};\, u = \frac{Q_r}{A_{i1}^i};\, A_{i1}^i = \pi\left(r_{i1}^i\right)^2;\, \phi = \frac{2\pi r_{i1}^o \Phi_{i1g}}{A_{i1}^i \rho^r c^r} \quad (51)$$

Choosing the following initial and boundary conditions according to

$$T(z,0) = T_s;\, T(0,t) = T_i;\, \frac{\partial T}{\partial z}(\infty,t) = 0 \quad (52)$$

the analytical solution (van Genuchten *et al.*, 1982) for Eq. 50 is given by

$$T(z,t) = T_i + \frac{T_s - T_i}{2}\left\{\begin{array}{l} \exp\left[\dfrac{(u-v)z}{2D}\right]erfc\left(\dfrac{z - vt}{2\sqrt{Dt}}\right) + \\ \exp\left[\dfrac{(u+v)z}{2D}\right]erfc\left(\dfrac{z + vt}{2\sqrt{Dt}}\right) \end{array}\right\} \quad (53)$$

$$v = u\sqrt{1 + \frac{4\phi D}{u^2}}$$

5

Diersch et al.

The numerical model is shown in Figure 3 forming a 3D box with a horizontal extent of 20 m x 20 m and a depth of 1 m. In the central position a single BHE is located, where the heat transfer coefficients of pipe-in to grout and grout to soil are identical $\Phi_{i1g} = \Phi_{sg}$, while the heat transfer of the pipe-out is set to zero $\Phi_{o1g} = 0$ to eliminate thermal interaction of the pipe-out to the grout heated by pipe-in.
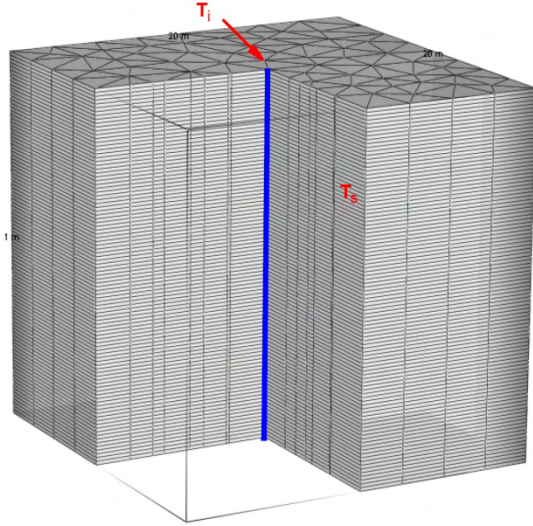

Figure 3: Single BHE in a 3D mesh (exaggerated cut view)
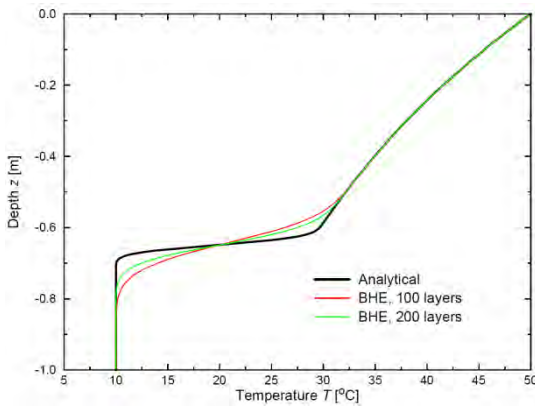
Figure 4: Computed temperature profiles in comparison to the analytical solution (with 100 and 200 layers, respectively) for the single pipe-soil interaction at $t = 0.02$ d

The computed temperature BHE profiles in comparison to the analytical solution at $t = 0.02$ days are shown in Figure 4, revealing a good agreement. As seen in Figure 4 at early times when the heat flow through the pipe is significantly influenced by advection a sufficient vertical spatial discretization is needed to obtain accurate solutions (compare the 100 vs. the 200 layer solution). At later times, however when the heat front in the pipe disappears and the process is dominated by heat transfer this effect declines.

2.6.2 BHE Solution Versus Fully Discretized 3D Model (FD3DM) Solution Applied to a Double U-Shape Pipe System

Comparisons between the proposed BHE solution and a fully discretized 3D model solution (FD3DM) are performed for heating operation of a 2U configuration located in central position of an aquifer domain measuring 20 m x 20 m in horizontal directions and 55 m in depth. The meshes used for both solutions are shown in Figure 5

revealing a much more refined tessellation for FD3DM to discretize appropriately the interior geometric structure of the 2U exchanger. In both meshes, however, the vertical discretization is the same by using 55 layers. For the 2U exchanger problem the used parameters are summarized in Table 1. In FD3DM 1D discrete feature (fracture) elements have been used to model the internal pipes. It was necessary to assign the inner pipe surplus to a high thermal conductivity of solid with anisotropy. For the surplus we took a value of $\lambda^s = 10^3$ J m^{-1}s^{-1} with an anisotropy factor of $\lambda^s_{zz} / \lambda^s_{xx,yy} = 0$.

Table 1: Parameters of the 2U Exchanger Problem

Parameter	Symbol	Value	Unit
Depth of borehole	$\bar{L}$	55	M
Borehole diameter	D	12	cm
Outer diameters of pipes-in	$d_{i1}{}^o$	3.2	cm
Outer diameters of pipes-out	$d_{o1}{}^o$	3.2	cm
Pipes-in wall thicknesses	b_{i1}, b_{i2}	2.9	mm
Pipes-out wall thicknesses	b_{o1}, b_{o2}	2.9	mm
Pipe distance	w	4.2	cm
Volumetric heat capacity of pipe walls	$\rho^p c^p$	$2.1574 \cdot 10^6$	J m^{-3} K^{-1}
Thermal conductivities of pipe walls	$\lambda_{i1}{}^p, \lambda_{i2}{}^p, \lambda_{o1}{}^p, \lambda_{o2}{}^p$	0.38	W m^{-1} K^{-1}
Total flow discharge of refrigerant	Q_r	38.284	m 3d −1
Total heat input rate	Q_h	$6.3242 \cdot 10^9$	J d−1
Reference temperature	T_o	R 10	°C
Inlet temperature	T_i	50	°C
Volumetric heat capacity of refrigerant	r c r	$4.12984 \cdot 10^6$	J m−3K−1
Thermal conductivity of refrigerant	r	0.65	J m^{-1}s^{-1}K^{-1}
Volumetric heat capacity of grout	$\rho^g c^g$	$2.19 \cdot 10^6$	J m^{-3}K^{-1}
Thermal conductivity of grout	λ^g	2.3	J m^{-1}s^{-1}K^{-1}
Porosity of soil	ε		
Volumetric heat capacity of groundwater	$\rho^f c^f$	$4.2 \cdot 10^6$	J m^{-3}K^{-1}
Volumetric heat capacity of soil	$\rho^s c^s$	$2.405 \cdot 10^6$	J m^{-3}K^{-1}
Thermal conductivity of groundwater	λ^f	0.65	J m^{-1}s^{-1}K^{-1}
Thermal conductivity of soil	λ^s	2.46	J m^{-1}s^{-1}K^{-1}
Longitudinal thermo-dispersivity of aquifer	α_L	0.5	m
Transverse thermo-dispersivity of aquifer	α_T	0.05	m
Initial temperature	Ts(0)	10	°C
Computed heat transfer coefficients:			
pipe-in to grout	Φ_{fig}	91.624	J m^{-2}s^{-1}K^{-1}
pipe-out to grout	Φ_{fog}	91.624	J m^{-2}s^{-1}K^{-1}
grout to grout 1	Φ_{gg1}	802.43	J m^{-2}s^{-1}K^{-1}
grout to grout 2	Φ_{gg2}	31.702	J m^{-2}s^{-1}K^{-1}
grout to soil	Φ_{gs}	181.02	J m^{-2}s^{-1}K^{-1}
Computed thermal resistances:			
pipe-in to grout	R_{fig}	0.1326	m s K J^{-1}
pipe-out to grout	R_{fog}	0.1326	m s K J^{-1}
grout to grout 1	R_{gg1}	0.02077	m s K J^{-1}
grout to grout 2	R_{gg2}	0.26287	m s K J^{-1}
grout to soil	R_{gs}	0.05861	m s K J^{-1}

A comparison of the BHE solutions to a fully discretized 3D model (FD3DM) is shown in Figure 6 for the short-term outlet temperature history, in Figure 7 for the long-time outlet temperature history and in Figure 8 for the vertical temperature profile after 12 hours. As revealed the agreement between the different solutions is quite good. For

long-term predictions the analytical BHE simulation has proved to be reasonably accurate and fast, while the numerical BHE computations became superior to the analytical BHE solution at short-term predictions and in good agreement with the FD3DM results from beginning.

For the FD3DM a forward Adams-Bashforth/backward trapezoid time integration scheme with a RMS error tolerance of 10^{-4} has been used. It took 276 time steps for the simulation period of 365 days. For the BHE solutions always a forward Euler/backward Euler time marching predictor-corrector scheme with a RMS error tolerance of 10^{-3} was preferred due to better robustness for this class of problems.

The analytical BHE required only 227 time steps. In contrast, the numerical BHE computations failed for the long-term run because the adaptive time step control could not increase the time steps anymore and a very large number of time steps would follow. Obviously, this is caused by random effects triggered from the stiff matrix system by poor numerical precision of the only 8 byte floating point mantissa.

The good agreement of the BHE solutions with the FD3DM results demonstrates the accuracy and practical applicability of the new BHE modeling strategy. Its numerical efficiency and capability will be more apparent for arrays of BHE.
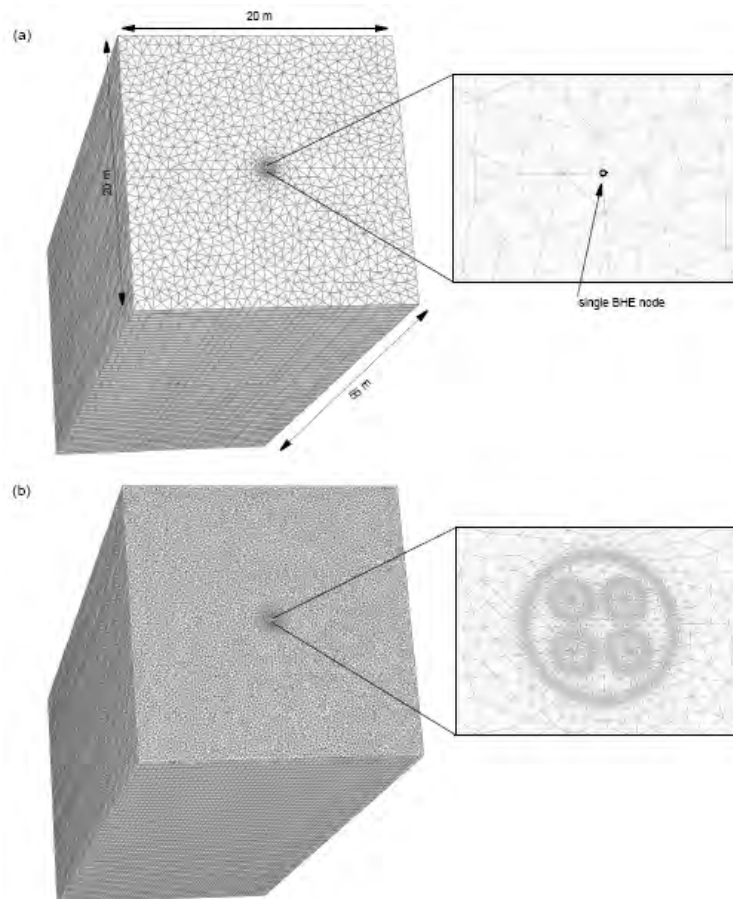

Figure 5: Finite-element meshes for (a) BHE consisting of 130.185 pentahedral elements and (b) FD3DM consisting of 1.204.665 pentahedral elements. Both meshes are vertically discretized by 55 layers
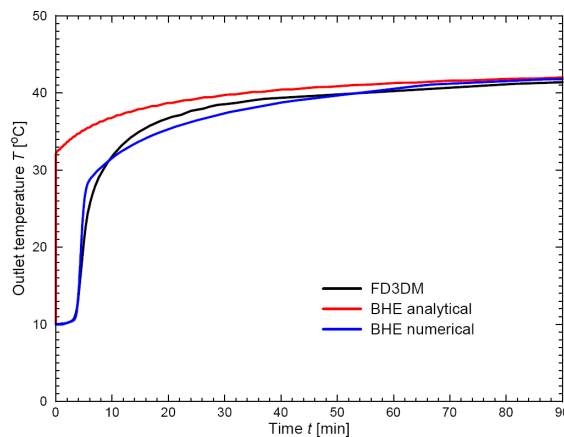

Figure 6: Short-term outlet temperature history of the BHE solution in comparison to the fully discretized 3D model (FD3DM) solution measured at the pipes' outlet
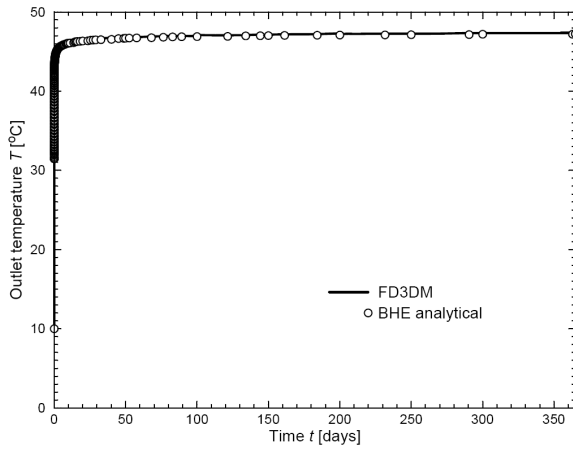
Figure 7: Long-term outlet temperature history of the BHE solution in comparison to the fully discretized 3D model (FD3DM) solution measured at the pipe's outlet
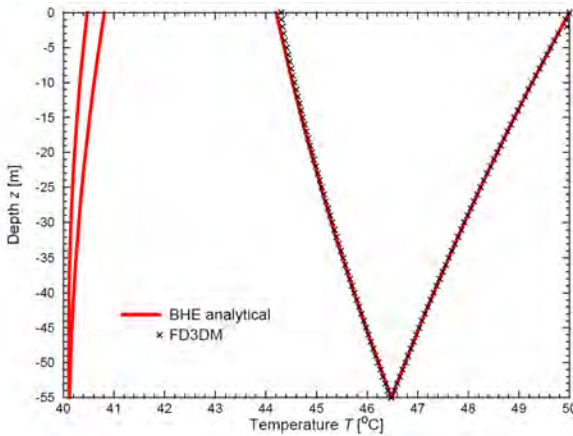

Figure 8: Analytical BHE solution of temperature profile at t = 12 hours in comparison to the fully discretized 3D model (FD3DM)

3. COUPLING OF FEFLOW WITH THE ENERGY SIMULATION CODE TRNSYS

Borehole thermal energy stores (BTES) consist of a large number of borehole heat exchangers typically installed with spacing in the range of two to five meters as the thermal interaction of the individual borehole heat exchangers is essential for an efficient storage process. BTES can be a reasonable technical and economical alternative – depending on the local geological and hydrogeological situation – to other techniques of heat storage for the use in solar assisted district heating systems with seasonal heat storage. BTES are very sensitive to groundwater flow. Both for permit procedures required by the authorities and for plant-engineering issues, a simulation tool is needed which is capable of predicting the three-dimensional temperature profile in the underground and the thermal efficiency of the store. Together with the new BHE option of FEFLOW the simulation of such installations is a feasible task.

In addition it is possible using a newly developed IFM module (ifm_trnsys) to couple the FEFLOW simulation with the energy simulation software TRNSYS (e.g. Bradley and Kummert, 2005). This way it is possible to model the complete energy transfer cycle for instance between an array of solar panels, the connected buildings and the subsurface heat storage system together with the thermal

interaction with the surrounding rocks. Ifm_trnsys uses FEFLOW's programmable interface API. The program allows an arbitrary number of BHE's which can be connected using arbitrary complex circuits. An example of the user interface is shown in Figure 9.
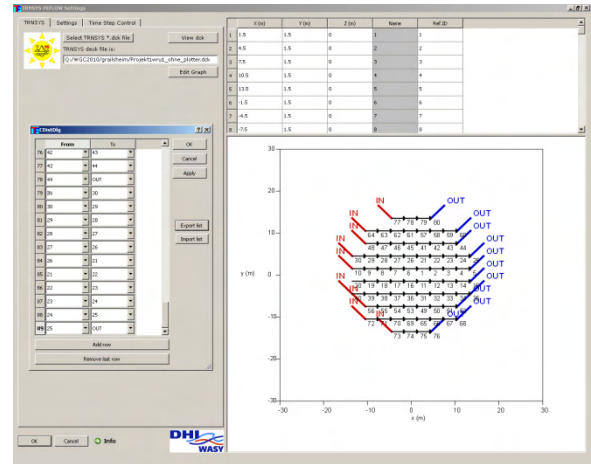

Figure 9: The user interface of the ifm_trnsys code for connecting the BHE array

A typical result of such computations is shown in Figure 10. However, the main model will be computed in the future.

CONCLUSIONS

A new finite-element analysis together with an analytic algorithm for the efficient computation of BHE systems has been implemented in FEFLOW by using a non-sequential solution strategy. First verification and benchmark calculations have shown good accuracy. Further tests with real data and field applications are currently in progress (e.g. Bauer et al., 2009). Furthermore, a direct coupling with the TRNSYS (Bradley and Kummert, 2005) code for energy simulation of buildings will be released shortly.
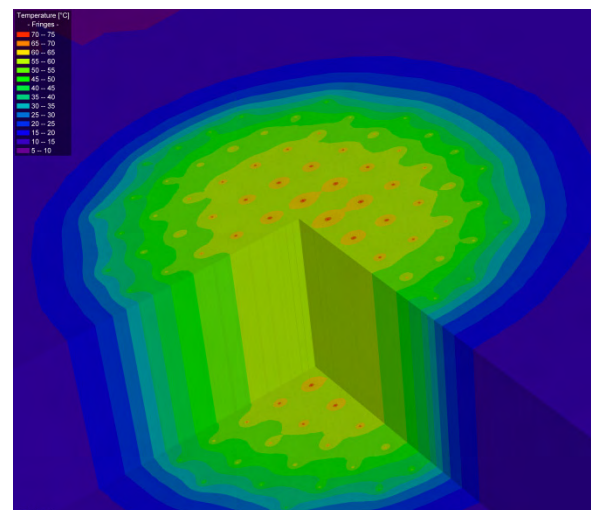

Figure 10: Temperature distribution around an array of 80 BHE computed with FEFLOW coupled with TRNSYS

REFERENCES

Al-Khoury, R., Bonnier, P. G. and Brinkgreve, R. B.: Efficient finite element formulation for geothermal heating systems. Part I: Steady state, *Int. J. Numer. Meth. Engng.* **63**(7), (2005), 988-1013.

Al-Khoury, R. and Bonnier, P. G.: Efficient finite element formulation for geothermal heating systems. Part II: Transient, *Int. J. Numer. Meth. Engng.* **67**(5), (2006), 725-745.

Bauer, D., Heidemann, W., Müller-Steinhagen, H. and Diersch, H.-J. G.: Modelling and simulation of groundwater influence on borehole thermal energy stores, Proceedings, Effstock 2009 - 11th International Conference on Energy Storage, Stockholm, Sweden (2009) in review.

Bradley, D. E. and Kummert, M.: New Evolutions in TRNSYS – A Selection of Version 16 Features; IBPSA (International Building Performance Simulation Association – World Conference) Conference Proceedings (2005).

Diersch, H.-J. G.: *Discrete feature modeling of flow, mass and heat transport processes by using FEFLOW.* FEFLOW's White Papers Vol. I, Chapter 9, WASY GmbH, Berlin (2002).

Diersch, H.-J. G. and Kolditz, O.: Variable-density flow and transport in porous media: approaches and challenges, Adv. Water Resour. **25**, (2002), 899-944.

Eskilson, P. and Claesson, J.: Simulation model for thermally interacting heat extraction boreholes. *Numerical Heat Transfer*, **13**, (1988), 149-165.

van Genuchten, M. Th. and Alves, W. J.: Analytical solutions of the one-dimensional convective-dispersive solute transport equation. *Technical Bulletin Number 1661,* 149p, US Dept. Agriculture (1982).

VDI-Gesellschaft Verfahrenstechnik und Chemieingenieurwesen: *VDI-Wärmeatlas: Wärme-übertragung bei der Strömung durch Rohre (heat transfer in flow through pipes).* Springer, 10. Auflage (2006).

Zienkiewicz, O. C. and Taylor, R. L.: *The finite element method. Volume 1: The basis.* 5th edition, Butterworth-Heinemann, Oxford (2000).

Zheng, C. (2007) FEFLOW: A finite-element ground water flow and transport modeling tool. ; reviewed by: Mike G. Trefry and Chris Muffels. 525–528. *Ground Water* **45** (5).